JCTC Journal of Chemical Theory and Computation

# 1-Fluoropropane. Torsional Potential Surface

Lionel Goodman* and Ronald R. Sauers

*Department of Chemistry and Chemical Biology, Wright and Rieman Laboratories, Rutgers, the State University of New Jersey, New Brunswick, New Jersey 08903*

Received August 15, 2005

**Abstract:** The systematic deletion of orbital interactions, using natural bond orbital (NBO) theory at the B3LYP/ 6-311++G(3df,2p) level, provides validation for the anti-C−H/C−F* hyperconjugative interaction providing the backbone for the gauche preference of 1-fluoropropane (FP). The FCCC torsional coordinate taking trans FP to gauche FP is predicted to be strongly contaminated by CCC bending with the result that a large part of the trans → gauche stabilization energy stems from mode coupling. The anti-C−H/C−F* hyperconjugative interaction is also found to play a major, if not determining, role in the coupling. The results of Rydberg deletion calculations suggest that Rydberg interactions play a role in NBO analysis, contrary to the usual assumption that interactions involving Rydberg orbitals can be ignored.

## I. Introduction

The term "gauche effect"[1] is frequently used for the counterintuitive conformational preference of polar group 1,2-disubstituted ethanes. The equilibrium conformer of 1,2-difluoroethane (DFE), for example, is the gauche geometry shown in Figure 1a, where the two fluorines are adjacent (with a FCCF dihedral angle ∼ 72°) to each other.[2] The gauche conformer is calculated to be approximately 0.8 kcal/mol more stable than the metastable trans conformer, where the fluorines are in anti orientation (Figure 1b). The gauche preference is counterintuitive since dipole repulsions between the polar C−F bonds and steric effects both favor the trans conformation. The accepted explanation for the gauche equilibrium geometry is based on $\sigma$ hyperconjugation involving charge transfer from C−H electron donor bonds to C−F* acceptor antibonds.[2,3] This type of orbital interaction is maximized when C−H bonds and C−F* antibonds are in anti orientation to each other. The consequence of the hyperconjugation model is that gauche conformational preference will be highly expressed for 1,2-disubstituted ethanes having two strongly electron-accepting substituents, as in 1,2-difluoroethane. This brings up the question of conformational preference in singly fluorine-substituted ethanes. A particularly interesting category is the 2-substituted 1-fluoroethanes, where maximal donor−acceptor interaction will depend on the $C_2$-X substituent bond electron-donating ability relative to both the $C_2$−H bond and their relative orientation. Rablen et al.[4] carried out an extensive study of the conformational preference and energetics of several 2-substituted 1-fluoroethanes and, in particular for the basic molecule, propane with a single fluorine substituent, 1-fluoropropane (FP; Figure 2). FP can be considered as a 2-substituted 1-fluoroethane with a methyl group in the 2 position. The conformational preference of FP is weakly gauche (by only 0.4 kcal/mol or less). Although Rablen's computations suggest that electrostatic attraction between fluorine and methyl strongly contributes to the gauche preference, they were not able to unambiguously establish the role of hyperconjugation. Since FP represents one of the simplest molecules exhibiting the gauche effect, its origin deserves detailed study for what it reveals about interactions leading to structural preference. We do this by using a feature

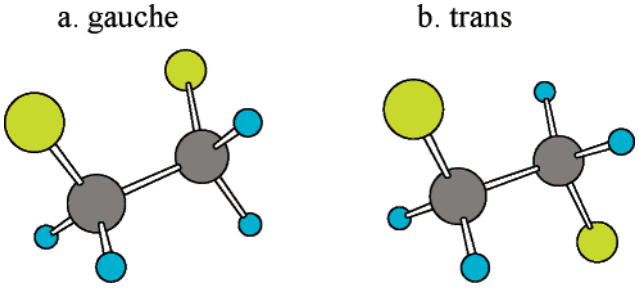


***Figure 1.*** 1,2-Difluoroethane conformers.

* Corresponding author. E-mail: goodman@rutchem.rutgers.edu.

10.1021/ct050204b CCC: $30.25 
Published on Web 10/11/2005

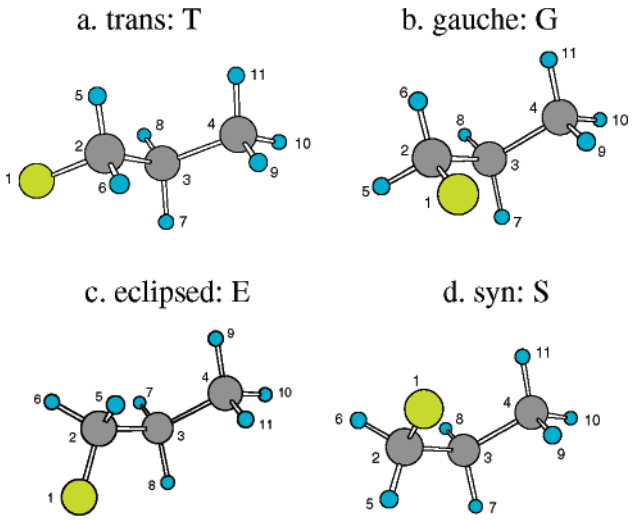


***Figure 2.*** 1-Fluoropropane conformers.

of natural bond orbital (NBO) theory[3,5] that allows the hyperconjugative interactions to be switched off.

Dipole−dipole repulsion is usually invoked as the interaction that forces the FCCF dihedral angle to 72° in DFE.[6] However, a recently proposed alternate rationalization for the >60° angle invokes both anti interactions, which maximize near 60°, and cis interactions, which maximize at a much larger dihedral angle.[2] The absence of dipole−dipole repulsion in FP provides an opportunity to further address conformational determinants in fluorohydrocarbons. The >3 kcal/mol G−T barriers are sufficient to regard FP as a semirigid molecule, but given the presence of several low lying torsional modes, we are persuaded to examine the role of mode coupling as a significant factor in determining the gauche preference energetics.

Microwave and infrared experiments[7] support FP's gauche conformational preference (Figure 2b) in accord with theoretical prediction.[4] The microwave-determined trans−gauche energy difference is 0.37 kcal/mol, larger than either the DFT- or CCSD(T)-calculated difference, however. The experimental barrier height (3.47 kcal/mol at the eclipsed geometry) is in reasonable agreement with Rablen's MP2 (3.89 kcal/mol) and our DFT calculations (given in the next section). The microwave-spectroscopy-determined FCCC dihedral angle is 62.6°, in close agreement with Rablen's calculated 62.2°, and in somewhat less agreement with our slightly larger DFT value (Section II). Despite the reasonable agreement between experiment and the levels of theory used in ref 4 and in this study, interesting questions remain. Why is the energetic preference for gauche over trans so much higher in DFE than in FP, despite the absence of gauche destabilizing dipole−dipole repulsion in FP? Rablen et al. raised the possibility that the gauche conformational preference actually could be largely due to electrostatic attraction between the negatively charged fluorine and the C−H bond of the methyl group in FP.[4] However, a hyperconjugation origin was not thoroughly investigated. In this paper, we will examine this possibility in detail.

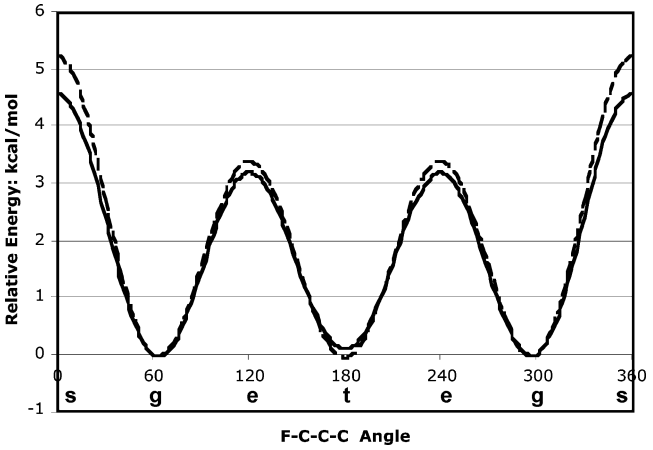


***Figure 3.*** Torsional potential energy curves for 1-fluoropropane showing dependence on the F−C−C−C dihedral angle. Fully relaxed rotation (solid curve); skeletal geometry frozen at trans geometry (dashed curve).

***Table 1.*** Energy of 1-Fluoropropane Conformers at Various Calculation Levels

| method | gauche (Hartrees) | trans[a] | eclipsed[a] | syn[a] |
|---|---|---|---|---|
| HF/6-311++G(3df,2p) | −217.194 033 | 0.016 | 3.70 | 4.99 |
| B3LYP/6-311++G(3df,2p) | −218.460 253 | 0.13 | 3.23 | 4.62 |
| MP4/6-311++G(3df,2p)[b] | −218.037 724 | 0.19 | 3.55 | 4.70 |
| CCSD(T) /6-311++G(2d,p)[b] | −218.035 210 | 0.19 | 3.53 | 4.67 |
| MP2/6-311++G(3df,2p) | −217.968 472 | 0.21 | 3.73 | 4.94 |
| MP2/6-31+G(d)[c] | | 0.38 | 3.85 | 5.26 |
| MP2/6-311++G**(6D)[c,d] | | 0.28 | 3.89 | 5.27 |

[a] Energy (kcal/mol) of fully optimized geometry relative to gauche conformer unless otherwise noted. [b] Single-point calculations at B3LYP/6-311++G(3df,2p) optimized geometry. [c] Rablen et al.[4] [d] Single-point energies at MP2/6-31+G(d).

## II. Torsional Potential Surface Landscape

The coordinate path between various conformers in FP can be usefully probed by FCCC dihedral angle rotation from 0° (for syn) through 60° (gauche) and 120° (eclipsed) to 180° (trans). Figure 3 shows the calculated[8] fully optimized potential surface in terms of the dihedral angle (solid curve). Both geometry optimization and energies were calculated at the B3LYP/ 6-311++G(3df,2p) level.[8] The potential surface landscape shows four features: a trans conformer (Figure 2a) at 180°, 0.13 kcal/mol higher than the equilibrium gauche conformer at 63.2° (Figure 2b), a prominent barrier (3.23 kcal/mol) between the trans and gauche conformers at the eclipsed geometry (119.9°; Figure 2c), and a still larger eclipsed-syn geometry barrier at 0° (Figure 2d), 4.62 kcal/mol above the gauche conformer. These are in qualitative agreement with both Rablen et al.'s MP2/6-311++G**(6D)[4] and Guirgis et al.'s MP2/6-311+G(2d,2p)[7b] single-point calculations. However, the smaller DFT gauche preference compared to that reported by Rablen's[4] 0.28−0.38 kcal/mol leads us to carry out additional calculations at different correlation levels. These are given in Table 1. Our results for single-point CCSD(T) calculations lead to an energy difference between the gauche and trans conformers of 0.19 kcal/mol, somewhat larger than the B3LYP value. In

***Table 2.*** 1-Fluoropropane B3LYP/6-311++G(3df,2p) Optimized Geometries[a]

| | gauche (G) | trans (T) | eclipsed (E) | syn (S) |
|---|---|---|---|---|
| | Skeletal Coordinates[b] | | | |
| $R$(C−F) | 1.400 | 1.398 | 1.401 | 1.399 |
| $R(C_2-C_3)$ | 1.514 | 1.514 | 1.531 | 1.541 |
| $R(C_3-C_4)$ | 1.528 | 1.530 | 1.529 | 1.531 |
| $\angle F-C_2-C_3$ | 110.44 | 110.37 | 110.60 | 111.86 |
| $\angle C_2-C_3-C_4$ | 113.55 | 111.79 | 113.63 | 114.34 |
| $\angle C_2-C_3-H_8$ | 107.24 | 108.74 | 106.96 | 108.86 |
| $\angle F-C_2-C_3-C_4$ | 63.18 | 180.00 | 120.03 | 0.02 |
| | C−H Coordinates | | | |
| $R(C_2-H_5)$ | 1.091 | 1.092 | 1.091 | 1.090 |
| $R(C_2-H_6)$ | 1.093 | 1.092 | 1.092 | 1.090 |
| $R(C_3-H_7)$ | 1.093 | 1.092 | 1.091 | 1.092 |
| $R(C_3-H_8)$ | 1.094 | 1.092 | 1.092 | 1.092 |
| $R(C_4-H_9)$ | 1.089 | 1.092 | 1.091 | 1.089 |
| $R(C_4-H_{10})$ | 1.090 | 1.090 | 1.090 | 1.090 |
| $R(C_4-H_{11})$ | 1.092 | 1.092 | 1.092 | 1.089 |

[a] See Figure 2 for conformer structure. [b] Bond lengths in Å, bond angles in degrees.

summary, these respectable high-level calculations lead to a gauche preference of only 0.1−0.3 kcal/mol.

## III. Coupling between Skeletal Motion and FCCC Dihedral Rotation

The nonrotational skeletal relaxations accompanying FCCC dihedral angle rotation are given in Table 2. Optimized geometries for the gauche and trans conformers show that the major skeletal relaxation between these conformers is the 1.8° ∠CCC decrease accompanying gauche → trans rotation. All other bond length and bond angle changes are insignificant (<0.003 Å and <0.1°). However, there are additional skeletal changes aside from the mentioned ones at the barrier maxima, occurring for the syn and eclipsed dihedral geometries; for example, the $C_2-C_3$ bond undergoes significant (0.02−0.03 Å) lengthening. Insight into the role that the nonrotational coordinates play in the potential surface features, in particular for the trans → gauche stabilization energy and for the G−T barrier at the eclipsed geometry, can be seen from two potential curves in terms of the FCCC dihedral angle given in Figure 3, one with frozen trans skeletal geometry (dashed curve), the other obtained from global optimized geometries (solid curve).

The landscape of both curves closely resemble each other, with three minima for 360° rotation and maxima at the 0° and 120° $F-C_2-C_3-C_4$ angles (see Figure 2). However, there is a significant effect on the T → G stabilization energy, $E_G-E_T$. Frozen rotation essentially obliterates the weak gauche preference, reversing the trans−gauche stabilization energy from 0.13 kcal/mol, gauche-conformer-preferred (for the fully optimized potential curve), to −0.014 kcal/mol, that is, a slight trans conformer preference (Table 3). On the other hand, the 3.2 kcal/mol fully relaxed trans → gauche barrier is only slightly increased. The largest energetic change is at the syn geometry: from 4.6 kcal/mol (fully relaxed) to 5.3 kcal/mol (rigid rotation). We conclude that skeletal relaxation, that is, the nonrotational phase space of the trans → gauche reaction path, plays an important role in the FP gauche preference. It is also a component of the syn barrier that cannot be ignored.

***Table 3.*** Relaxation Effects on the Conformer Energies (kcal/mol)

| | relaxation[a] | | |
|---|---|---|---|
| | $E_G-E_T$ | $E_E-E_T$ | $E_S-E_T$ |
| fully relaxed | −0.13 | 3.10 | 4.49 |
| rigid[b] | 0.014 | 3.42 | 5.28 |
| | partial relaxation[c] | | |
| all bond lengths | −0.003 | 3.29 | 4.88 |
| all bond angles | −0.089 | 3.25 | 4.77 |
| $R(C_2-C_3)$ | −0.013 | 3.29 | 4.88 |
| $\angle C_2-C_3-C_4$ | −0.094 | 3.35 | 4.92 |
| $\angle C_2-C_3-C_4 + R(C_2-C_3)$ | −0.094 | 3.23 | 4.74 |
| $\angle C_2-C_3-H_8$ | −0.016 | 3.50 | 5.42 |

[a] Skeletal relaxation accompanying FCCC dihedral angle rotation. [b] All skeletal coordinates are held at frozen trans geometry. [c] All other skeletal coordinates are held at frozen trans geometry.

To obtain further insight into the energetic consequences of relaxation, we decompose the full skeletal relaxation into two categories: (1) angular and (2) bond length relaxations. The results, given in Table 3, show that it is the angular ones that are primary.

Parsing of the skeletal angular relaxations, where only one angle is allowed to relax from its trans description and the other coordinates are frozen, is also given in Table 3. Partially relaxed rotations allow insight into the roles that individual internal coordinates play in trans−gauche energetics, and Table 2 shows that the paramount angular relaxation is ∠CCC scissor opening. This motion represents the largest amplitude oscillation in the 313 $cm^{-1}$ gauche conformer "scissor" vibrational mode, and Table 3 clearly demonstrates that the coupling of dihedral torsion to this mode provides the major relaxation effect on G−T energetics.

## IV. Hyperconjugation Model

The link between hyperconjugation and the gauche effect can be validated by removing all the electron charge transfers from bonds and lone pairs to antibond NBOs and Rydberg orbitals. The results of these single-point calculations at the gauche, trans, eclipsed, and syn geometries are given in Table 4, and the potential curve at 10° FCCC dihedral angle intervals is given in Figure 4. When all hyperconjugative interactions are switched off (dashed curve in Figure 4), the potential curve is inverted from that for the real molecule (solid curve). There still are two energy minima, but these occur at the eclipsed and syn geometries rather than at trans and gauche, which are now maxima. Furthermore, the B3LYP/6-311++G(3df,2p) energy of the gauche conformer is 0.5 kcal/mol higher than that of the trans instead of lower; the most stable structures are now syn and eclipsed, with eclipsed the strongly preferred conformer. The important conclusion: inversion of the potential curve from that of the real molecule when hyperconjugation is deleted clearly establishes that hyperconjugation is an essential part of the machinery driving the FP gauche preference. An interesting ancillary conclusion, not revealed in Table 4, is that the

***Table 4.*** Deletion Effects on Conformer Energies (kcal/mol)

| hyperconjugative deletion | T conformer deletion energy change[a] | G−T deletion difference | E−T deletion difference | S−T deletion difference |
|---|---|---|---|---|
| all hyperconjugation | 117.4 | 0.46 | −3.72 | −2.10 |
| all vicinal | 116.0 | −0.96 | −2.56 | −2.90 |
| all geminal | 17.7 | −0.64 | 4.46 | 4.78 |
| all remote | 2.5 | −0.53 | 2.30 | 4.07 |

[a] *E*(after deletion) − *E*(total).

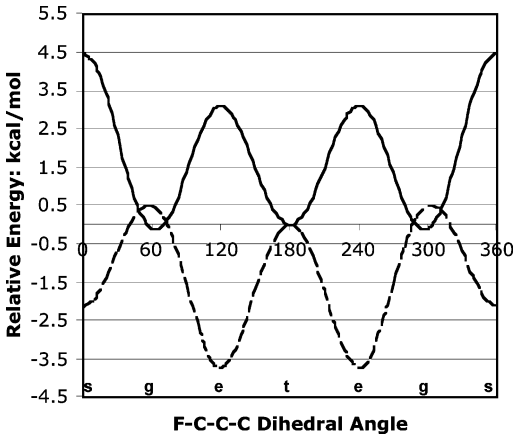


***Figure 4.*** Potential energy curves for 1-fluoropropane showing the effect of orbital interaction. Full Hamilton, full optimization (solid curve); all hyperconjugative interactions deleted (dashed curve). Both curves have the zero-energy reference point at the 180° trans geometry.

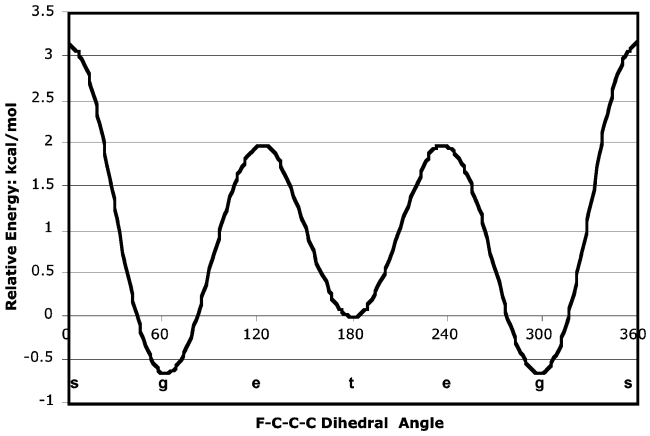


***Figure 5.*** Torsional potential-energy curve for 1-fluoropropane with all geminal hyperconjugative interactions deleted using full Hamiltonian optimized geometry.

energies of both the syn and eclipsed structures are less affected by hyperconjugation deletion than those of the gauche and trans.

The removal of only the geminal hyperconjugations (e.g., $C_2-H_5/C_2-F^*$) leaves the lowest-energy FP conformer unchanged from gauche (Figure 5 and Table 4). Thus, geminal interactions, which include such bond/antibond charge transfers as $C_2-H_5/C_2-C_3^*$ and $C-F/C_2-H_5^*$, have little influence on the gauche geometry of the preferred conformer, but they do have a strong effect on syn and eclipsed energetics (Table 4).

However, when all vicinal hyperconjugations alone are removed, the landscape of the completely deleted hyperconjugations case is retained (Figure 6); the maxima are again at trans and gauche. There is also a parallel with the no-hyperconjugation calculation of Figure 4 in that the energies of the syn and eclipsed structures are less affected by vicinal hyperconjugation deletion than those of the gauche and trans. The consequence is that the deepest energy minima are (as in the all-hyperconjugation deletion case) at the syn and eclipsed geometries. But, surprisingly, as in the full Hamiltonian calculation, the gauche energy is lower than the trans.

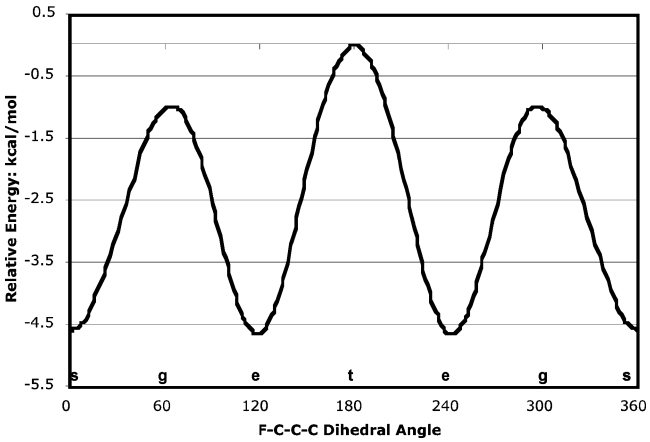


***Figure 6.*** Torsional potential energy curve for 1-fluoropropane with all vicinal hyperconjugative interactions deleted. Single-point calculations using full Hamiltonian optimized geometry.

One additional interaction category remains: remote hyperconjugations between bonds, fluorine lone pairs (lp), and distant antibonds such as $C_4-H_{10}/C-F^*$ and $F(lp)/C_3-H_8^*$. The deletion of all 36 possible remote interactions has only small effects on the conformer energies and does not change the preferred conformation. It remains gauche (Table 4). Thus, systematic deletion calculations establish that only the removal of vicinal hyperconjugative interactions leads to potential-curve inversion. The surprising result of vicinal deletion, that gauche energy is lower than that of trans, is discussed further in Section VI.

The vicinal interactions can be further parsed into anti ($C_3-H_7/C-F^*$) and cis (e.g., $C_3-H_8/C-F^*$) orbital interactions. Their relative importance can be ascertained by separate deletions, retaining all other vicinal interactions. For the gauche conformer, cis interaction deletion raises the energy by only 0.81 kcal/mol, compared to 5.63 kcal/mol for anti deletion. The anti interaction does not occur in the trans conformer; both interactions are now cis. Deletion of the two possible cis interactions in this conformer raises the energy by 1.32 kcal/mol, the magnitude of each cis interaction remaining essentially unchanged from its value in

***Table 5.*** Deletion Energies Generated by Rigid Rotation from trans Conformer (kcal/mol)

| hyperconjugative deletion | T conformer deletion energy change[a] | G−T deletion difference | E−T deletion difference | S−T deletion difference |
|---|---|---|---|---|
| all hyperconjugaton | 117.4 | 0.45 | −1.44 | 1.98 |
| all vicinal | 116.0 | −1.12 | −2.62 | −1.53 |
| all geminal | 17.6 | −0.58 | 2.66 | 4.50 |

[a] *E*(after deletion) − *E*(total).

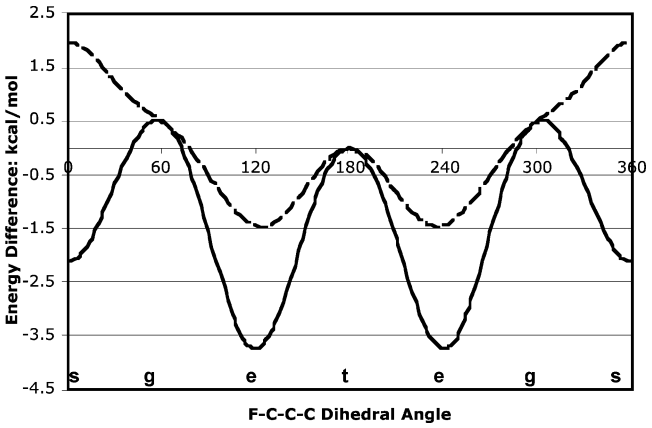


***Figure 7.*** Potential-energy curves with all hyperconjugative interactions deleted. Optimized geometry (solid curve); frozen at trans skeletal geometry (dashed curve). Both curves have the zero-energy reference point at the 180° trans geometry.

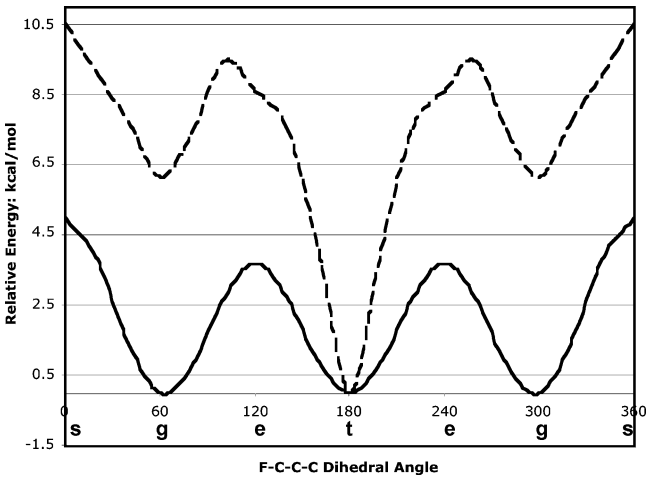


***Figure 8.*** Energy curves for 1-fluoropropane. Full Hamiltonian potential curve (solid line); steric exchange repulsion single-point calculations (dashed line). Both curves utilize HF/6-311++G(3df,2p) wave functions and have the zero-energy reference point at the 180° trans geometry.

gauche. The clear conclusion is that the anti interaction is much greater (nearly 7 times greater) than that of the cis. This disparity is much larger than in 1,2-difluoroethane, where an account of both types of interactions is necessary to understand the gauche−trans potential surface.[2] The overarching conclusion is that the anti orbital hyperconjugative interaction provides the backbone for the gauche effect in FP.

Because of the importance of skeletal relaxation to the T−G stabilization energy (see Section III), it is instructive to obtain the hyperconjugation deletion energies for rigid rotation, thereby eliminating changes in skeletal bond lengths and angles. The results of these calculations referenced to the frozen trans optimized geometry are given in Table 5. The same general pattern for deletions with and without relaxation (i.e., vicinal interactions are more important than geminal ones, as expected from local symmetry considerations) and the inversion of trans and gauche conformer energetics by extinguishing hyperconjugation interactions are obtained. The clear outcome: the determinant controlling the G and T orbital interactions is the rotation itself, even though the torsional coordinate is contaminated by skeletal displacements.

However, Figure 7 shows that the landscape for the rigid rotation potential curve with all hyperconjugated interactions quenched is considerably different from the fully relaxed equivalent (also shown in the same figure); the pronounced gauche geometry maximum in the fully relaxed curve disappears in the rigid rotation curve. Most significant is that the disparities in the two curves largely relate to the eclipsed and syn conformers, where the effect of excluding hyperconjugation interactions in the rigid rotation case reverses the S−T energy difference found for relaxed rotation. Thus, the conclusion that the G and T orbital interaction energies are primarily determined by torsional rotation is diluted for the E and, even more so, the S interaction energies.

## V. Steric Exchange Repulsion Model

Steric exchange repulsion is classically defined as the effect of Pauli exchange repulsion, a short-range force, which spatially separates pairs of electrons. The conceptual foundation of NBO steric analysis can be found in several publications by Weinhold[9−11] showing that quantitative appreciation of total steric exchange repulsion for a given molecular geometry can be obtained from the energy difference between orthogonal natural localized molecular orbital (NLMOs) and nonorthogonal preorthogonal natural localized molecular orbital (PNLMOs) descriptions of the molecular wave function. The PNLMOs and NLMOs are closely related to preNBOs (PNBOs) and NBOs with somewhat different localizations designed to improve exchange repulsion quantifications.[11]

The dashed curve in Figure 8 represents the calculated HF/6-311++G(3df,2p) total steric exchange repulsion at 20° intervals using the NBO steric analysis, described above. (A B3LYP repulsion plot is almost identical to the HF one; however, the HF curve is conceptually better founded.) A striking feature of the repulsion plot is the decreased repulsion at the trans geometry. There is also a much less pronounced decrease near the gauche geometry. These features allow the conclusion that lowered steric exchange

***Table 6.*** Rydberg Deletion Effects on Conformer Energies (kcal/mol)

| hyperconjugative deletion | T conformer deletion energy change[a] | G−T deletion difference | E−T deletion difference | S−T deletion difference |
|---|---|---|---|---|
| all Rydberg[b] | 49.6 | −0.38 | 0.95 | 2.09 |
| only vicinal valence[c] | 61.8 | 0.65 | −2.03 | −0.55 |

[a] *E*(after deletion) − *E*(total). [b] Valence interactions remain. [c] Only vicinal Rydberg interactions remain.

repulsion plays a major if not determining role in stabilizing the metastable 180° trans conformer. Moreover, the maxima at the syn and eclipsed FCCC dihedral angles strongly suggest that the syn and eclipsed geometry maxima in the potential curve (solid curve in Figure 8) arise at least in part from steric repulsion.

As seen from the comparison of repulsion values at the gauche and trans dihedral angles in Figure 8, the effect of shutting off steric exchange repulsion would be to greatly increase the gauche−trans preference, a consequence of greater exchange repulsion destabilization of the gauche conformer. The clear conclusion is that exchange repulsion does not play a significant role in forming the FP gauche conformational preference over the trans. However, it plays an important role in stabilizing the gauche conformer relative to the eclipsed.

## VI. Discussion

An interesting conundrum that arises from the systematic deletion calculations pointed out in Section IV is that, even with all-vicinal interactions deleted, the energy of the gauche conformer remains lower than trans—opposite to that found for complete hyperconjugation removal. The well-respected Brunck−Weinhold[3] rules for gauche conformer preference link vicinal hyperconjugative interactions to gauche preference, and their deletion is predicted to change the preference to trans. To address this problem, we separate the vicinal interactions involving Rydberg orbitals from those involving valence orbitals by restoring the Rydberg interactions into the all-vicinal interactions deletion calculation. The outcome of this new calculation, now deleting only vicinal *valence* interactions, is that the gauche conformer becomes less energetically favorable than the trans (Table 6). If the complete hyperconjugation deletion removal ("no-star") calculation is modified so that only Rydberg orbitals are deleted (i.e., interactions involving the antibond valence orbitals are restored), the gauche conformer becomes more energetically favorable than the trans (Table 6).

In a sense, these calculations are illegal because Rydberg orbitals are brought into the NBO scheme to ensure orbital orthogonality; thus, vicinal deletion excluding Rydberg orbitals is equivalent to deleting nonorthogonal PNBO vicinal antibonds.[10] Deletion of only the Rydberg orbitals has a similar flavor since it is equivalent to a full PNBO deletion calculation. Since a tenet of NBO analysis is that the extra valence natural atomic orbitals in the Rydberg basis play practically no significant role in the theory,[10] these energy inversions provide a challenge. One of the most dramatic and characteristic simplifying features of NBO analysis is that they can effectively be ignored.[10]

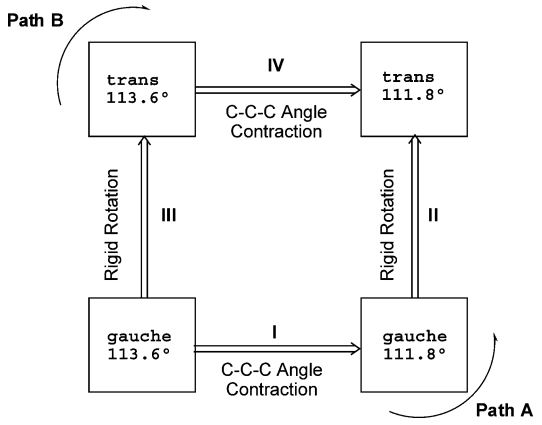


***Figure 9.*** Stepwise analysis of $C_2C_3C_4$ angular contraction energetics for the gauche equilibrium conformation. Step I: angular contraction leading to a prepared state with the trans-$C_2C_3C_4$ angle. Step II: rigid rotation from the prepared state leading to partially relaxed *trans*-1-fluoropropane. Step III: rigid rotation of the equilibrium gauche conformer leading to *trans*-1-fluoropropane with gauche skeletal geometry. Step IV: $C_2C_3C_4$ angular contraction of the prepared trans state leading to partially relaxed *trans*-1-fluoropropane.

The relaxation studies described in Section III demonstrate that the gauche preference is linked to the CCC angle in the propane skeleton of FP, evidenced by expansion of the 111.8° CCC angle in the trans conformer to 113.6° in the gauche (Table 2). A facile explanation for the CCC angle opening in the gauche conformer is that it reduces increased repulsion from the fluorine lone pairs to the $C_4$−H bonds. Although we show in Sections IV and V that the stereoelectronic origin of the gauche preference comes from hyperconjugative attractive electronic effects, which depend primarily on the FCCC dihedral angle, it remains to obtain insight into the underlying factors affecting the CCC angle as part of the dihedral angle rotation process.

To do this, we focus on separate considerations of Pauli exchange, Lewis energy,[12] and hyperconjugation for two alternate CCC angle-contracting paths for FCCC dihedral rotation from the gauche conformer, shown in Figure 9. One path (path A) first contracts the CCC angle in the optimized gauche conformer (113.6°) to its calculated value in the trans (111.8°), step I. There is no dihedral rotation in step I; that is, the 111.8 °CCC angle (with all other bond lengths and angles frozen to their values in the gauche equilibrium conformer) represents a prepared state of the gauche conformer. Step II is a dihedral rotation step from the prepared gauche state to a partially relaxed trans geometry. Path B starts with frozen dihedral rotation (step III) from the gauche conformer (all geometrical parameters remain those of the gauche conformer), ending in a 113.6° ∠CCC prepared state of the trans conformer. Step IV contracts the

***Table 7.*** Energy Contributions for 1-Fluoropropane Rigid Rotation/Angular Relaxation (kcal/mol)[a]

| step | $\Delta E_{exch}$ | $\Delta E_{deloc}$ | $\Delta E_{Lewis}$ | $\Delta E_{total}$ |
|---|---|---|---|---|
| I | 1.68 | −0.14 | 0.23 | 0.089 |
| II | −2.94 | −0.48 | 0.55 | 0.074 |
| III | −2.07 | −0.49 | 0.73 | 0.24 |
| IV | 0.81 | −0.12 | 0.04 | −0.079 |

[a] $\Delta E_{exch}$, $\Delta E_{deloc}$, and $\Delta E_{Lewis}$ refer to exchange repulsion, delocalization, and Lewis energy changes, respectively, for steps I−IV in Figure 9. $\Delta E_{exch}$ is calculated as the energy difference between occupied (orthogonal) NLMOs and the associated preorthogonal (Pauli Principle violating) PNLMOs; $\Delta E_{deloc}$ represents the energy change attributed to electron transfer from nearly doubly occupied (bonding) orbitals to nearly vacant (antibonding) orbitals; $\Delta E_{Lewis}$ refers to the energy of NBOs with ≅2 occupancy and can be associated to the localized electron pairs of the Lewis structure.

CCC angle in the trans prepared state to its value in the fully optimized trans conformer, with all other geometrical parameters remaining frozen. The associated energy changes accompanying paths A and B are shown in Table 7.

An analysis of the total energy changes in Table 7 shows an increase on going to the prepared state of step I and a decrease for step IV, as expected. Our first focus is on the exchange repulsion changes: $\Delta E_{exch}$ strongly increases (1.7 kcal/mol) for the CCC angle contraction occurring in step I but shows a much smaller increase (0.8 kcal/mol) for the same angular contraction in step IV. Thus, although exchange repulsion increases upon CCC angular contraction in both the equilibrium gauche and prepared trans states, it increases much less in the prepared trans one. We conclude that the angular expansion that accompanies the T → G rotational process does relieve the increased exchange repulsion occurring in the gauche conformation.

Different behavior is found for $\Delta E_{deloc}$, the delocalization energy change. It is slightly stabilizing (−0.14 kcal/mol) for step I, CCC angular contraction of the gauche conformer, and almost identically so (only −0.12 kcal/mol) in step IV, angular contraction of the prepared trans state. This identity leads to the conclusion that hyperconjugative interactions are not selectively linked to the CCC angular expansion in the gauche conformer.

Additional interest is found in the change in Lewis energy for step I. The Lewis structure of a molecule can be defined in an NBO representation by nearly doubly occupied bonding orbitals and lone pairs, without the delocalization effects of conjugation and hyperconjugation; $E_{Lewis} = E_{total} - E_{deloc}$. $E_{Lewis}$ then is linked to changes in bond strength. The 0.23 kcal/mol increase for step I shows that the Lewis structure of the prepared gauche state is destabilized relative to the equilibrium gauche conformer. In terms of the bond strengths, the contracted angle of the prepared state represents an unfavorable geometry. Thus, in contrast to the behavior of $\Delta E_{exch}$, there does not appear to be a link between $\Delta E_{Lewis}$ and the CCC angular contraction on going to the trans geometry.

Even though overall hyperconjugative interaction does not appear to link to the CCC angle change between the G and T conformers, there does appear to be a link to the CCC angle. This is exposed in Figure 10 by comparison of the expunged anti-C−H/C−F* interaction and full Hamiltonian

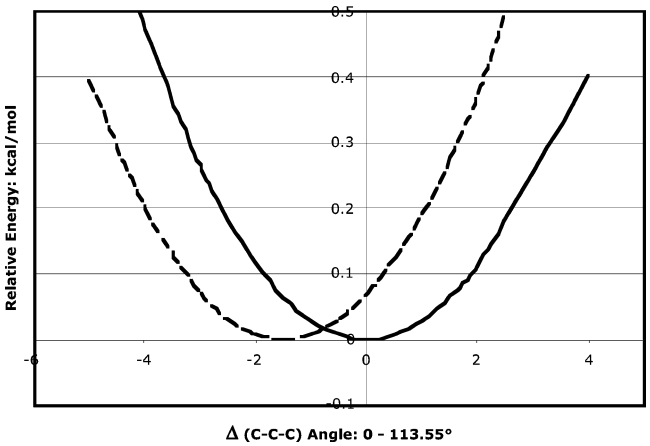


***Figure 10.*** Potential energy curves for C−C−C angular expansion at fixed gauche geometry. Full Hamiltonian (solid curve); deletion of anti-C−H/C−F* interactions (dashed curve).

energy curves versus the CCC angle for the gauche conformer. The point of this comparison is that the potential minima represent the change in gauche conformer geometry when only anti-C−H/C−F* hyperconjugation is absent, thus, giving the needed chemically insightful smoking gun otherwise buried in the full hyperconjugation deletions. The shift in minima demonstrate that the CCC angle is decreased by ∼1.7° when the anti-C−H/C−F* interaction is removed. This provides the needed insight into the 1.8° opening of the CCC angle on going from the trans conformer (where there are no anti-C−H/C−F* orbital interactions) to the gauche one. The effect of this interaction in the gauche conformer is to increase the CCC angle close to the global optimization increase.

Our overall conclusion is that both increased exchange repulsion and increased delocalization accompany CCC angle expansion in the T → G reaction path, with consequent preferential stabilization of the more-open angle gauche conformer. It is difficult to reliably assess which of these two interactions is primary, but on the basis of Figure 10, the attractive factor appears to be more important.

## VII. Conclusions

Because FP is an example of an elementary molecule exhibiting a gauche effect (without the complication of dipole−dipole repulsion), it is of considerable importance to study it thoroughly. The DFT/ab initio calculations on 1-fluoropropane conformational preference and torsional potential surface reported here and NBO analysis all provide insight into the conformational preference machinery and provide thought-provoking results on the role of Rydberg orbitals in NBO analysis. We emphasize that the approach taken in this study is the systematic deletion of interaction types (lone-pair/$\sigma^*$ hyperconjugations, steric repulsion, etc.) and not the comparison of calculated relative magnitudes of these interactions. In this sense, the deletion-caused inversions of the potential-curve landscape represent a kind of truth table and avoid quantitative pitfalls of NBO analysis.[13]

Our deletion calculations provide convincing validation for the anti-C−H/C−F* hyperconjugative interaction providing the backbone for the gauche effect in FP. The cis orbital

interaction is found to be much less important than in 1,2-difluoroethane. Thus, cis interactions, unlike in 1,2-difluoroethane, are not linked to the FP equilibrium conformer 63° FCCC dihedral angle.

Geometry optimization predicts that a ~2° expansion of the CCC angle is the major important skeletal change in the T → G reaction coordinate. A detailed analysis shows that both increased hyperconjugative attraction and decreased exchange repulsion at the larger angle account for the angle opening.

Finally, the results of Rydberg orbital deletion calculations, while not altering any of our overall conclusions concerning stereoelectronic interactions in FP, do not support the supposition that Rydberg interactions can be ignored in NBO analysis. We intend to pursue this aspect of Rydberg orbital participation in a future study.

**Acknowledgment.** We thank Vojislava Pophristic, Paul R. Rablen, Frank Weinhold, and Kenneth B. Wiberg for many helpful comments on the manuscript.

## References

(1) Wolfe, S. *Acc. Chem. Res.* **1972**, *5*, 102−111.

(2) Goodman, L.; Gu, H.; Pophristic, V. *J. Phys. Chem. A* **2005**, *109*, 1223−1229 and references therein.

(3) Brunck, T. K.; Weinhold, F. *J. Am. Chem. Soc.* **1979**, *101*, 1700−1709.

(4) Rablen, P. R.; Hoffmann, R. W.; Hrovat, D. A.; Borden, W. T. *J. Chem. Soc., Perkin Trans. 2* **1999**, 1719−1726 and references therein.

(5) Weinhold, F. In *The Encyclopedia of Computational Chemistry*; Schleyer, P. v. R., Allinger, N. L., Clark, T., Gasteiger, J., Kollman, P. A., Schaefer, H. F., III, Schreiner, P. R., Eds.; John Wiley & Sons: Chichester, U. K., 1998; pp 1792−1811.

(6) Trindle, C.; Crum, P.; Douglass, K. *J. Phys. Chem. A* **2003**, *107*, 6236−6242.

(7) (a) Hayashi, M.; Fujitake, M. *J. Mol. Struct.* **1986**, *146*, 9−24. (b) Guirgis, G. A.; Zhu, X.; Durig, J. R. *Struct. Chem.* **1999**, *10*, 445−461.

(8) *Gaussian 98*, revision A.11.2; Frisch, M. J., Trucks, G. W., Schlegel, H. B., Scuseria, G. E., Robb, M. A., Cheeseman, J. R., Zakrzewski, V. G., Montgomery, J. A., Jr., Stratmann, R. E., Burant, J. C., Dapprich, S., Millam, J. M., Daniels, A. D., Kudin, K. N., Strain, M. C., Farkas, O., Tomasi, J., Barone, V., Cossi, M., Cammi, R., Mennucci, B., Pomelli, C., Adamo, C., Clifford, S., Ochterski, J., Petersson, G. A., Ayala, P. Y., Cui, Q., Morokuma, K., Rega, N., Salvador, P., Dannenberg, J. J., Malick, D. K., Rabuck, A. D., Raghavachari, K., Foresman, J. B., Cioslowski, J., Ortiz, J. V., Baboul, A. G., Stefanov, B. B., Liu, G., Liashenko, A., Piskorz, P., Komaromi, I., Gomperts, R., Martin, R. L., Fox, D. J., Keith, T., Al-Laham, M. A., Peng, C. Y., Nanayakkara, A., Challacombe, M. W., Gill, P. M., Johnson, B., Chen, W., Wong, M. W., Andres, J. L., Gonzalez, C., Head-Gordon, M., Replogle, E. S., Pople, J. A., Eds.; Gaussian, Inc.: Pittsburgh, PA, 2001.

(9) (a) Badenhoop, J. K.; Weinhold, F. *J. Chem. Phys.* **1997**, *107*, 5406−5421. (b) Badenhoop, J. K.; Weinhold, F. *J. Chem. Phys.* **1997**, *107*, 5422−5432.

(10) Glendening, E. D.; Badenhoop, J. K.; Reed, A. E.; Carpenter, J. E.; Weinhold, F. *NBO 5.0*; Theoretical Chemical Institute, University of Wisconsin: Madison, WI, 2002.

(11) Reed, A. E.; Weinhold, F. *J. Chem. Phys.* **1985**, *83*, 1736−1740.

(12) Suidan, L.; Badenhoop, J. K.; Glendening, E. D.; Weinhold, F. *J. Chem. Educ.* **1995**, *72*, 583−586.

(13) Salzner, U.; Schleyer, P. v. R. *Chem. Phys. Lett.* **1992**, *190*, 401−406.

CT050204B